Short-Circuit Constrained Distribution Network Reconfiguration Considering Closed-Loop Operation

Leonardo H. Macedo[1,*], Juan M. Home-Ortiz[1], Renzo Vargas[2], José R. S. Mantovani[1], Rubén Romero[1], João P. S. Catalão[3]

[1] *Department of Electrical Engineering, São Paulo State University, Avenida Brasil 56, Centro, 15385-000, Ilha Solteira, SP, Brazil*

[2] *Center for Engineering, Modeling and Applied Social Sciences, Federal University of ABC Santo André, Avenida dos Estados 5001, Bairro Santa Terezinha, 09210-580, Santo André, SP, Brazil*

[3] *FEUP and INESC TEC Porto, R. Dr. Roberto Frias, 4200-465, Porto, Portugal*

Abstract

This paper presents a novel scenario-based stochastic mixed-integer second-order cone programming model to solve the problem of optimal reconfiguration of distribution systems with renewable energy sources considering short-circuit constraints. The proposed formulation minimizes technical losses by modifying the statuses of sectionalizing and tie switches, allowing the operation of distribution networks with radial and closed-loop topologies. Since the formation of loops could impact fault current levels, short-circuit constraints are considered in the problem formulation. Numerical experiments are carried out using an 84-node system and the results demonstrate the effectiveness of the proposed formulation to reduce technical losses notably when a closed-loop operation is allowed. Additionally, it is verified that short-circuit constraints prevent the adoption of network configurations with high short-circuit values.

Keywords: Closed-loop operation; distribution network reconfiguration; renewable energy sources; short-circuit; stochastic programming.

Nomenclature

Indices and sets:

i, j	Indices for nodes
ij, ji	Indices for branches
c	Index for a short-circuit scenario
s	Index for stochastic scenarios
Ω_B	Set of branches
$\Omega_{\mathcal{B}}$	Set of branches for short-circuit calculations
Ω_C	Set of short-circuit scenarios
Ω_{DG}	Set of nodes with distributed generators (DGs)
Ω_N	Set of nodes
$\Omega_{\mathcal{N}}$	Set of nodes for short-circuit calculations

*Principal corresponding author

E-mail addresses: leohfmp@ieee.org (Leonardo H. Macedo), juan.home@unesp.br (Juan M. Home-Ortiz), renzo.vargas@ufabc.edu.br (Renzo Vargas), mant@dee.feis.unesp.br (José R. S. Mantovani), ruben.romero@unesp.br (Rubén Romero), catalao@fe.up.pt (João P. S. Catalão).

Ω_S	Set of stochastic scenarios
Ω_{SS}	Set of substations (SSs) nodes
Parameters:	
$\mathcal{C}_s^E$	Energy price of a stochastic scenario
$\overline{I}_{ij}$	Current capacity of a branch
$\overline{I}_{ij,c}^{CC}$	Short-circuit current limit for a branch on a short-circuit scenario
M^V, M^Θ	Big-M parameters
N^{LP}	Maximum number of basic loops allowed
$P_{i,s}^D$, $Q_{i,s}^D$	Active/reactive power demands
$\underline{PF}_i^{DG}$, $\overline{PF}_i^{DG}$	Power factor limits of a DG
R_{ij}, X_{ij}, Z_{ij}	Resistance, reactance, and impedance of a branch
$\overline{P}_i^{DG}$	Installed DG capacity
$\overline{S}_i^{DG}$	Apparent power capacity of a DG
$\overline{S}_i^{SS}$	Apparent power capacity of a SS
$\overline{V}$, $\underline{V}$	Maximum/minimum voltage magnitude limits
$\tilde{V}_{i,s}$	Estimate of the voltage magnitude
Δ_s^T	Duration of a stochastic scenario
$\Phi_{i,s}^{DG}$	Generation factor of a DG unit
Continuous variables:	
$\imath_{ij,s}^{SQ}$	Square of the current magnitude on a branch
$\hat{\imath}_{ij,c}^{R}$, $\hat{\imath}_{ij,c}^{I}$	Real/imaginary parts of the current on a branch on a short-circuit scenario
$\hat{\imath}_{i,c}^{R^{SS}}$, $\hat{\imath}_{i,c}^{I^{SS}}$	Real/imaginary parts of the current injected by a SS on a short-circuit scenario
$\hat{\imath}_{i,c}^{R^{F}}$, $\hat{\imath}_{i,c}^{I^{F}}$	Real/imaginary parts of the short-circuit current at a faulted node in a short-circuit scenario
$p_{ij,s}$, $q_{ij,s}$	Active/reactive power flows through a branch
$p_{i,s}^{DG}$, $q_{i,s}^{DG}$	Active/reactive power injected by a DG
$p_{i,s}^{SS}$, $q_{i,s}^{SS}$	Active/reactive power injected by a SS
$v_{i,s}^{SQ}$	Square of the voltage magnitude at a node
$\hat{v}_{i,c}^{R}$, $\hat{v}_{i,c}^{I}$	Real/imaginary parts of the voltage at a node on a short-circuit scenario
f_{ij}	Fictitious flow on a branch
g_i	Fictitious generation at SS nodes
$\delta_{ij,c}^{R}$, $\delta_{ij,c}^{I}$	Slack variable for the real/imaginary parts of the voltage drop on a branch on a short-circuit scenario
$\theta_{i,s}$	Voltage angle at a node
$\lambda_{ij,s}^{V}$	Slack variable for the voltage drop calculation
$\lambda_{ij,s}^{\theta}$	Slack variable for the angle difference calculation
Binary variables:	
w_{ij}^{SW}	Operational state of a branch

1. Introduction

Conventionally, electric power distribution networks are planned to have a weakly-meshed structure but are operated with a radial topology [1]. The adoption of radial structures responds to various technical reasons including the simplification of the protection system coordination and the reduction of short-circuit current values [2], [3]. However, in recent years, the closed-loop operation has been considered as an alternative to radial topologies due to operational advantages [4], [5]. For instance, in a normal state, a weakly-meshed configuration reduces technical losses [3], improves the reliability of distribution systems [6], and increases the hosting capacity of renewable energy sources (RES) in distribution networks [5], [7], [8]. On the other hand, the creation of loops during the restorative state improves the system's response to permanent faults by rearranging more de-energized loads to adjacent feeders [9].

One of the most common approaches to improve the operation of distribution systems is by performing network reconfiguration. It consists of changing the topology of the network through switching operations for alleviating congestions, reducing losses, and improving the voltage profile while, typically, maintaining a radial configuration for the system [10], [11], [12], [13].

An alternative to the radial operation is to allow the formation of loops in the network. In [4], a genetic algorithm-based approach is presented for solving the optimal power flow problem in a real Czech urban closed-looped distribution network. In [5], the authors present a comparison between closed-loop alternatives and network reinforcement solutions to increase distributed generation connection to a real French network. Reference [3] presents a mixed-integer nonlinear programming (MINLP) model for the reconfiguration problem allowing a significant decrease in losses with a reduced number of closed-loops. However, the formation of loops in distribution networks should be taken into account in the fault calculation as this type of configuration could impact fault current levels [5], [6].

Electric distribution networks are exposed to short-circuit faults that can cause undesirable

conditions to consumers and damage to utilities' equipment. Fault current levels depend on many factors, including network topology, grounding arrangements, and the number of in-service distributed generators (DGs) [14]. DGs have different contributions to a fault current depending on the technology of the generation unit. In general, synchronous and induction generators have high contributions to fault current levels, however inverter-based units' contribution to a fault could be neglected due to disconnection speed [14]. Short-circuit constraints are considered in this work to avoid network topologies that can present high values of short-circuit currents, such as when different substations (SSs) are interconnected [6]. Note that, even for radial configurations, short-circuit constraints should be considered in the reconfiguration problem. However, this type of constraint is widely ignored in the literature [10], [15]. To the best of the authors' knowledge, no paper has yet presented a mathematical optimization model taking into account short-circuit constraints in the distribution network reconfiguration problem.

In this work, we consider network reconfiguration for reducing technical losses of distribution systems with RES. The proposed approach considers opening sectionalizing switches to provide more flexibility to the network operation. Uncertain parameters, such as renewable generation availability, energy prices, and loads are represented through stochastic scenarios. Moreover, short-circuit constraints are considered in the problem so that the resulting configurations can be formed without compromising the isolation levels of equipment. The proposed formulation consists of a new scenario-based stochastic mixed-integer second-order cone programming (MISOCP) model. To handle the uncertainties of RES, a stochastic scenario-based formulation is used. Tests are performed using an 84-node distribution system.

The main contributions of this work are as follows:

- From a modeling perspective, a new stochastic programming-based model is proposed to determine the optimal network topology to improve the operation of distribution systems taking into account short-circuit limits of the network's assets.

- From a methodological perspective, the resulting mixed-integer nonlinear programming problem is recast in order to obtain a relaxed MISOCP model that is treatable, scalable, and can be effectively solved by off-the-shelf optimization solvers.

The remainder of this paper is organized as follows: the mathematical formulation of the problem is presented in Section 2; the tests with the 84-node system and a discussion of the results are shown in Section 3; finally, the conclusions of the work are presented in Section 4.

2. Mathematical Formulation

2.1 Objective Function

The objective function of the problem, presented in (1), minimizes the total cost of the energy losses.

$$\text{minimize} \sum_{\forall ij \in \Omega_B} \sum_{s \in \Omega_S} \mathcal{C}_s^E \Delta_s^T R_{ij} \boldsymbol{i}_{ij,s}^{SQ} \tag{1}$$

Note that (1) considers the values of the losses for all branches in all operating scenarios, multiplied by the corresponding duration of the scenario and the energy price in the scenario. Alternative objectives can also be considered in the formulation, such as improving the voltage regulation of the system, balancing the load among the substations, or increasing the hosting capacity of the network for renewables.

2.2 Power Flow Constraints

The ac operation of the distribution system is represented by the power flow equations (2)–(8) [16].

$$\sum_{ji \in \Omega_B} p_{ji,s} - \sum_{ij \in \Omega_B} \left(p_{ij,s} + R_{ij} \boldsymbol{i}_{ij,s}^{SQ} \right) + p_{i,s}^{SS} + p_{i,s}^{DG} = P_{i,s}^{D} \tag{2}$$

$$\sum_{ji \in \Omega_B} q_{ji,s} - \sum_{ij \in \Omega_B} \left(q_{ij,s} + X_{ij} \boldsymbol{i}_{ij,s}^{SQ} \right) + q_{i,s}^{SS} + q_{i,s}^{DG} = Q_{i,s}^{D} \tag{3}$$

$$\forall i \in \Omega_N, s \in \Omega_S$$

$$v_{i,s}^{SQ} - v_{j,s}^{SQ} + \lambda_{ij,s}^{V} = 2(R_{ij}p_{ij,s} + X_{ij}q_{ij,s}) + Z_{ij}^{2}\ell_{ij,s}^{SQ} \tag{4}$$

$$\tilde{V}_{i,s}\tilde{V}_{j,s}(\theta_{i,s} - \theta_{j,s} + \lambda_{ij,s}^{\theta}) = X_{ij}p_{ij,s} - R_{ij}q_{ij,s} \tag{5}$$

$$v_{j,s}^{SQ}\ell_{ij,s}^{SQ} \geq p_{ij,s}^{2} + q_{ij,s}^{2} \tag{6}$$

$$\left|\lambda_{ij,s}^{V}\right| \leq M^{V}(1 - w_{ij}^{SW}) \tag{7}$$

$$\left|\lambda_{ij,s}^{\theta}\right| \leq M^{\Theta}(1 - w_{ij}^{SW}) \tag{8}$$

$$\forall ij \in \Omega_B, s \in \Omega_S$$

Constraints (2) and (3) are the active and reactive power balance equations, respectively, that represent the application of Kirchhoff's current law to the system. Constraints (4)–(8) represent the application of Kirchhoff's voltage law to the system, in which (7) and (8) are used to calculate the slack variables $\lambda_{ij,s}^{V}$ and $\lambda_{ij,s}^{\theta}$ according with the statuses of the switches. Note that (6) is a second-order cone constraint. Ideally, this constraint should be active in the solution, otherwise, the terms $R_{ij}\ell_{ij,s}^{SQ}$, $X_{ij}\ell_{ij,s}^{SQ}$, and $Z_{ij}^{2}\ell_{ij,s}^{SQ}$ in (2), (3), and (4) will be overestimated, resulting in higher values of losses. Note, however, that the active power losses are minimized in the objective function (1), leading (6) to remain active.

2.3 Physical and Operational Limits of the System

The physical and operational limits of the system are considered in constraints (9)–(13).

$$0 \leq \ell_{ij,s}^{SQ} \leq \overline{I}_{ij}^{2} w_{ij}^{SW} \qquad \forall ij \in \Omega_B, s \in \Omega_S \tag{9}$$

$$\left|p_{ij,s}\right| \leq \overline{VI}_{ij} w_{ij}^{SW} \qquad \forall ij \in \Omega_B, s \in \Omega_S \tag{10}$$

$$\left|q_{ij,s}\right| \leq \overline{VI}_{ij} w_{ij}^{SW} \qquad \forall ij \in \Omega_B, s \in \Omega_S \tag{11}$$

$$\underline{V}^{2} \leq v_{i,s}^{SQ} \leq \overline{V}^{2} \qquad \forall i \in \Omega_N, s \in \Omega_S \tag{12}$$

$$(p_{i,s}^{SS})^{2} + (q_{i,s}^{SS})^{2} \leq \left(\overline{S}_{i}^{SS}\right)^{2} \qquad \forall i \in \Omega_{SS}, s \in \Omega_S \tag{13}$$

Constraint (9) represents the current limits for the branches according to the status of the switches, while (10)–(11) are the active and reactive power limits for the branches, also dependent on the status of the switches. Constraint (12) is the voltage magnitude limit for the nodes. Finally, constraint (13) is the apparent power capacity of the SSs.

2.4 Renewable DGs

The operational limits of the renewable DGs are shown in (14)–(16).

$$(p_{i,s}^{DG})^2 + (q_{i,s}^{DG})^2 \leq \left(\overline{S}_i^{DG}\right)^2 \qquad \forall i \in \Omega_{DG}, s \in \Omega_S \tag{14}$$

$$0 \leq p_{i,s}^{DG} \leq \Phi_{i,s}^{DG} \overline{P}_i^{DG} \qquad \forall i \in \Omega_{DG}, s \in \Omega_S \tag{15}$$

$$-p_{i,s}^{DG} \tan(\cos^{-1}(\underline{PF}_i^{DG})) \leq q_{i,s}^{DG} \leq p_{i,s}^{DG} \tan(\cos^{-1}(\overline{PF}_i^{DG})) \tag{16}$$

$$\forall i \in \Omega_{DG}, s \in \Omega_S$$

Constraint (14) represents the power generation capacity of the DGs. Constraint (15) limits the active power of the renewable DGs according to the availability of the renewable resource. Finally, constraint (16) limits the power factor of the DGs.

2.5 Topological Constraints

The connectivity of the system and the maximum number of loops allowed to be formed are controlled by (17)–(20) through artificial demands that must be attended at all nodes.

$$|\Omega_N| - |\Omega_{SS}| \leq \sum_{ij \in \Omega_B} w_{ij}^{SW} \leq |\Omega_N| - |\Omega_{SS}| + N^{LP} \tag{17}$$

$$\sum_{ji \in \Omega_B} f_{ji} - \sum_{ij \in \Omega_B} f_{ij} + g_i = 1 \qquad \forall i \in \Omega_N \tag{18}$$

$$\left|f_{ij}\right| \leq |\Omega_N| w_{ij}^{SW} \qquad \forall ij \in \Omega_B \tag{19}$$

$$0 \leq g_i \leq |\Omega_N| \qquad \forall i \in \Omega_{SS} \tag{20}$$

Constraint (17) limits the maximum number of basic loops allowed to be formed in the system. This constraint operates together with (18)–(20), which ensure the connectivity of the system, by requiring that there must be a path from each node of the system to a SS. For the load nodes ($\Omega_N \backslash \Omega_{SS}$), $g_i = 0$.

2.6 Short-Circuit Constraints

Changes in the network topology due to reconfiguration and the formation of loops affect the voltage profile and the currents of the system in normal operation scenarios, as well as the short-circuit currents in fault scenarios. It must be guaranteed that the reconfiguration of the network will not produce an increase of the short-circuit currents beyond the short-circuit capacity of the protective devices. Moreover, it is desirable to produce only small changes in the short-circuit currents, so that the coordination of the protection is not overly affected.

The following considerations are made for the short-circuit analysis:

i. The SS is represented by a power source with a voltage of $1\angle 0°$ p.u. in series with an equivalent impedance of the upstream network [17];

ii. The inverter-interfaced renewable DG does not contribute to the short-circuit currents [14];

iii. A single fault at a node is considered in each fault scenario, and the faults are symmetrical three-phase short-circuits [17];

iv. Since short-circuit currents are much larger than the load currents in steady-state, the loads are ignored in the calculation of the short-circuit currents [17].

The short-circuit constraints, with considerations (i)–(iv), are presented in (21)–(27).

$$\sum_{ji \in \Omega_{\mathcal{B}}} \hat{i}^{R}_{ji,c} - \sum_{ij \in \Omega_{\mathcal{B}}} \hat{i}^{R}_{ij,c} + \hat{i}^{R^{SS}}_{i,c} = \hat{i}^{R^{F}}_{i,c} \tag{21}$$

$$\sum_{ji \in \Omega_{\mathcal{B}}} \hat{i}^{I}_{ji,c} - \sum_{ij \in \Omega_{\mathcal{B}}} \hat{i}^{I}_{ij,c} + \hat{i}^{I^{SS}}_{i,c} = \hat{i}^{I^{F}}_{i,c} \tag{22}$$

$$\forall i \in \Omega_{\mathcal{N}}, c \in \Omega_C$$

$$\hat{v}^R_{i,c} - \hat{v}^R_{j,c} + \delta^R_{ij,c} = R_{ij}\hat{i}^R_{ij,c} - X_{ij}\hat{i}^I_{ij,c} \tag{23}$$

$$\hat{v}^I_{i,c} - \hat{v}^I_{j,c} + \delta^I_{ij,c} = X_{ij}\hat{i}^R_{ij,c} + R_{ij}\hat{i}^I_{ij,c} \tag{24}$$

$$\left|\delta^R_{ij,c}\right| \leq 2\overline{V}(1 - w^{SW}_{ij}) \tag{25}$$

$$\left|\delta^I_{ij,c}\right| \leq 2\overline{V}(1 - w^{SW}_{ij}) \tag{26}$$

$$\left(\hat{i}^R_{ij,c}\right)^2 + \left(\hat{i}^I_{ij,c}\right)^2 \leq \left(\overline{I}^{CC}_{ij,c}\right)^2 w^{SW}_{ij} \tag{27}$$

$$\forall ij \in \Omega_{\mathcal{B}}, c \in \Omega_C$$

In (21)–(27), the set $\Omega_{\mathcal{B}}$ contains the branches of Ω_B and the additional branches with the equivalent impedance of the upstream network connected to the SS buses; the set $\Omega_{\mathcal{N}}$ contains the nodes of Ω_N and the terminal nodes of the additional branches from $\Omega_{\mathcal{B}} \backslash \Omega_B$; finally, Ω_C is the set of fault scenarios. A fault at a single node is considered in each fault scenario.

Constraints (21) and (22) are the application of Kirchhoff's current law to the real and imaginary components of the short-circuit currents. Constraints (23)–(26) represent the application of Kirchhoff's voltage law to the system in the fault scenarios. Finally, constraint (27) is the limit for the short-circuit current on a branch according to the fault scenario and the status of the branch. These values must also be limited by the isolation levels of the equipment installed in the network. It should be noted that, in each fault scenario, the voltage at the faulted node is set to zero in the model.

Note that the short-circuit constraints presented in this paper allow changes in the network topology, differently from [17], which considers a short-circuit model for pre-defined fixed topologies. Moreover, the formulation (21)–(27) can be applied to networks considering both traditional and modern digital protective devices that can be reparametrized. For the latter, it is possible to obtain more flexibility in the solutions. However, the isolation levels of the equipment present in the network must also be taken into account when these devices are considered.

In the proposed scenario-based formulation, the objective function (1) is linear, as well as constraints (2)–(5), (7)–(12), and (15)–(26). Constraint (6) is a second-order cone, while (13),

(14), and (27) are quadratic constraints. Due to the presence of the binary variable w_{ij}^{SW}, the resulting formulation is a stochastic MISOCP model, which can be solved by off-the-shelf optimization solvers.

3. Tests and Results

The proposed model is tested using the 84-node system, adapted from [18], shown in Fig. 1, which operates at 11.40 kV. This system has four 600 kW photovoltaic (PV) generation units with inductive and capacitive power factor limits of 0.9 at nodes 9, 24, 42, and 64. The minimum and maximum voltage magnitude limits are 0.93 and 1.05 p.u., respectively. For a radial operation, the system has 13 normally open switches. It is assumed that every branch has a switch. Complete data for the system is available in [19].

The solar irradiations, energy prices, and power demands are represented using a set of 16 stochastic scenarios obtained from historical data and reduced using the *k-means* method [20].

The proposed formulation was implemented in AMPL [21] and solved with the commercial solver CPLEX v20.1.0 [22] on a computer with a 3.2 GHz Intel® Core™ i7–8700 processor and 32 GB of RAM.

3.1 Study Cases

Considering the initial topology presented in Fig. 1, the solution of the proposed model disregarding network reconfiguration provides the short-circuit current values of the system considering a fault at each node connected to a substation node, i.e., faults are considered at nodes 1, 11, 15, 25, 30, 43, 47, 56, 65, 73, and 77, one at a time, in each fault scenario. Based on these short-circuit currents, the study cases proposed in Section 3.3 allow controlled variations, from 1% until 25%, in the short-circuit current values, $\overline{I}_{ij,c}^{CC}$, to find topologies with lower costs of the energy losses. These short-circuit values are also limited by the isolation levels of the equipment.

The proposed model is solved considering the two approaches presented below:

- *Case I – without network reconfiguration:* Starting with the initial radial configuration, it is only allowed to close tie (normally-open) switches, while opening sectionalizing (normally-closed) switches is disregarded, as considered in [8];
- *Case II – with network reconfiguration:* The reconfiguration process considers both closing tie switches and opening sectionalizing switches.

The following subsection presents the results obtained with the proposed model for both approaches and disregarding the short-circuit constraints, (21)–(27), in the model.

3.2 Results Without Considering Short-Circuit Constraints

Disregarding any switching operation, the initial configuration shown in Fig. 1, with the switches of branches 5-55, 7-60, 11-43, 12-72, 13-76, 14-18, 16-26, 20-83, 28-32, 29-39, 34-46, 40-42, and 53-64 open, has a total annual cost of the energy losses of US$ 104,569.30.

Table I summarizes the main results obtained for the problem without considering short-circuit constraints. When disregarding the short-circuit constraints, (21)–(27), of the model, the optimal radial configuration, obtained with $N^{LP} = 0$, presents a total annual cost of the energy losses of US$ 92,957.95, with 13 switches of branches open. This represents a cost reduction of 11.10% in comparison with the initial configuration.

For Case I, only allowing closing switches and disregarding the short-circuit constraints, the optimal configuration, obtained with $N^{LP} = 13$, i.e., allowing the formation of up to 13 basic loops, presents a total annual cost of the energy losses of US$ 92,070.36, with 4 switches of branches open. This represents a cost reduction of 11.95% in comparison with the initial configuration, while 9 loops are formed in the system.

For Case II, allowing network reconfiguration and closed-loop operation and disregarding the short-circuit constraints, the optimal configuration, obtained with $N^{LP} = 13$, presents a total annual cost of the energy losses of US$ 91,375.26, with 8 switches of branches open. This represents a cost reduction of 12.62% in comparison with the initial configuration, while 5 loops are formed in the system.

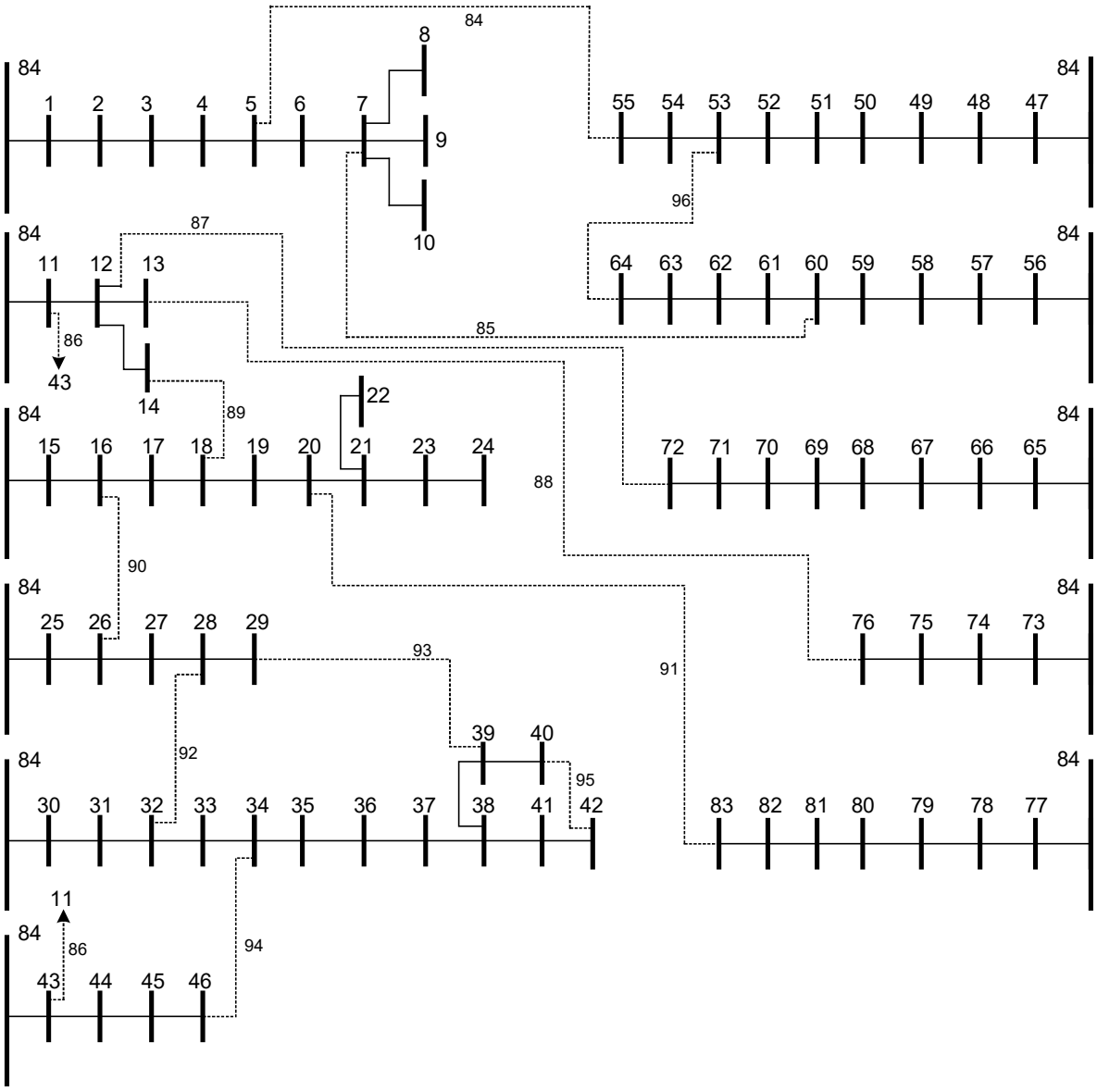

Figure 1: Initial configuration of the 84-node system.

Table I: Results without considering short-circuit constraints

Case	Objective function value (US$)	Open switches	Number of loops
I	104,569.30	5-55, 7-60, 11-43, 12-72, 13-76, 14-18, 16-26, 20-83, 28-32, 29-39, 34-46, 40-42, 53-64	0
II	92,957.95	6-7, 12-13, 33-34, 37-38, 39-40, 62-63, 71-72, 82-83, 5-55, 11-43, 14-18, 16-26, 28-32	0
I	92,070.36	11-43, 14-18, 28-32, 29-39	9
II	91,375.26	12-13, 32-33, 37-38, 39-40, 81-82, 5-55, 11-43, 14-18	5

Note that, from the results of Cases I and II, not necessarily an all-closed-switches solution presents the lowest value of losses. Indeed, by closing all switches in the system, its operation becomes infeasible, since the current capacities of branches 43-84 and 44-45 are violated in some operation scenarios.

The following subsection presents the results obtained with the proposed model for both approaches and considering variations of the maximum value of the short-circuit current limits, obtained from the initial configuration.

3.3 Results Considering Short-Circuit Constraints

First, we consider the maximum short-circuit current on a branch in a fault scenario, $\overline{I}_{ij,c}^{CC}$, the short-circuit current value obtained from the initial configuration. Then, we allow maximum deviations, from 1% up to 25% (also limited by the isolation levels of the equipment), in these values for obtaining solutions that comply with the isolation levels of equipment and try to maintain the coordination of the protection.

Fig. 2 presents the summary of the solutions obtained for Cases I and II for the values of maximum short-circuit current deviations: Fig. 2(a) presents the annual cost of the energy losses for each solution, while Fig. 2(b) presents the number of basic loops in the corresponding solution. It can be observed, in Fig. 2(a), that by allowing higher values for the maximum value of the short-circuit current deviation, it is possible to obtain solutions with lower values of the annual cost of energy losses for both Cases I and II. Moreover, since Case II allows for more flexibility than Case I, the solutions for Case II will always present lower (or in the worst-case equal) values of the annual cost of energy losses than the solutions for Case I.

Moreover, from Fig. 2(b), it is possible to conclude that, by increasing the value of the maximum short-circuit current deviation, it is possible to form more loops in the system or to obtain different network configurations that allow reducing the annual cost of energy losses.

Table II summarizes the main results obtained for the problem considering short-circuit constraints. For a maximum short-circuit current deviation of 1%, in Case I, the topology of the system does not change and remains equal to the initial configuration. For Case II, the corresponding solution has a cost of US$ 101,159.96, with 13 switches of branches open, and presents a radial configuration. This represents a cost reduction of 3.26% in comparison to the solution of Case I.

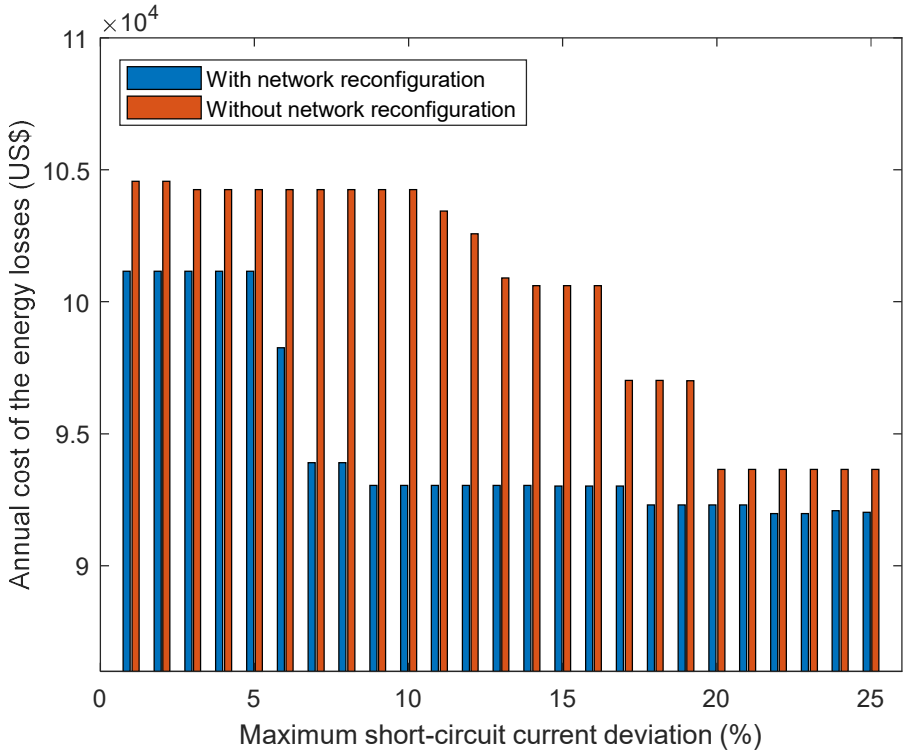

(a)

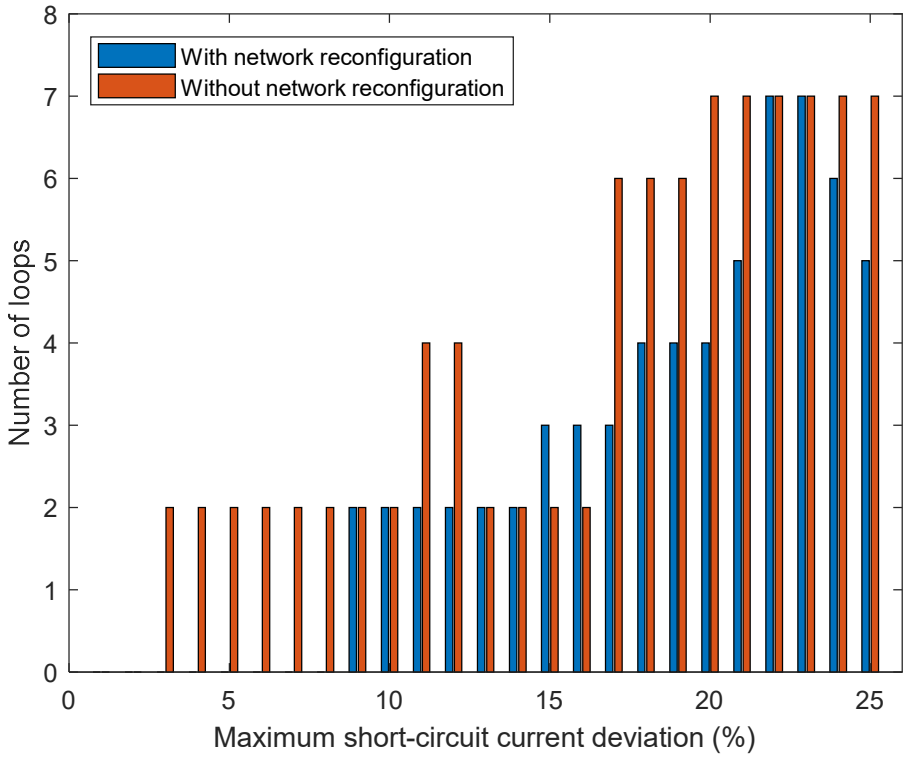

(b)

Figure 2: (a) Annual costs of energy losses obtained by changing the maximum short-circuit deviation in relation to the initial configuration and (b) the corresponding numbers of loops in the system for each solution.

Table II: Solutions considering short-circuit constraints

Case	Maximum short-circuit current deviation (%)	Objective function value (US$)	Open switches	Number of loops
I	1	104,569.30	5-55, 7-60, 11-43, 12-72, 13-76, 14-18, 16-26, 20-83, 28-32, 29-39, 34-46, 40-42, 53-64	0
II	1	101,159.96	6-7, 36-37, 38-41, 54-55, 60-61, 75-76, 11-43, 12-72, 14-18, 16-26, 20-83, 28-32, 34-46	0
I	9	104,255.70	5-55, 7-60, 11-43, 13-76, 14-18, 16-26, 20-83, 28-32, 29-39, 34-46, 53-64	2
II	9	93,041.95	6-7, 12-13, 32-33, 35-36, 38-39, 60-61, 81-82, 5-55, 11-43, 16-26, 28-32	2
I	25	93,644.96	5-55, 11-43, 13-76, 14-18, 16-26, 28-32	7
II	25	92,024.57	12-13, 33-34, 38-39, 82-83, 5-55, 11-43, 14-18, 16-26	5

For a maximum short-circuit current deviation of 9%, in Case I, a solution with a total annual cost of the energy losses of US$ 104,255.70 is obtained, in which 11 switches of branches are open, and 2 basic loops are formed in the system. For Case II, the corresponding solution has a cost of US$ 93,041.95, with 11 switches of branches open, and, again, 2 basic loops are formed. The solution for Case II represents a cost reduction of 10.76% in comparison to the solution of Case I.

Finally, for a maximum short-circuit current deviation of 25%, in Case I, a solution with a total annual cost of the energy losses of US$ 93,644.96 is obtained, in which 6 switches of branches are open, and 7 basic loops are formed in the system. For Case II, the corresponding solution has a cost of US$ 92,024.57, with 8 switches of branches open, and 5 basic loops formed. The solution for Case II represents a cost reduction of 1.73% in comparison to the solution of Case I.

It can be verified that by increasing the values of the maximum deviations in the short-circuit currents, it is possible to obtain solutions with lower energy losses costs. From an optimization problem perspective, this can be explained by the larger feasible region that is obtained with higher maximum short-circuit current values. This allows us to obtain solutions with lower costs of energy losses. From the power system operation perspective, by allowing larger values of short-circuit currents, it is possible to obtain more flexible configurations for the network operation, allowing, for example, the interconnection of substations and the formation of more loops

Table III: Performance tests considering a maximum short-circuit current deviation of 7%

Number of stochastic scenarios	Number of short-circuit scenarios	CPU time (s)
16	0	1636
16	3	6261
16	8	7463
16	11	22183
1	11	901
4	11	4184
8	11	14495
12	11	17318

in the system. Note that, a system with more loops may present lower values of normal operation currents on branches and, consequently, lower values of energy losses. However, the short-circuit currents of meshed systems are usually higher, especially when substations are interconnected [6].

The results indicate that the approach considered in Case II is capable of providing better solutions than the approach in Case I, reducing the total annual cost of the energy losses in the system while maintaining adequate levels of the short-circuit currents. Note that, by allowing a maximum deviation of the short-circuit current in the system of 9%, it is possible to obtain a solution that is only 0.71% worse than the solution for the problem without considering short-circuit constraints. For the solution obtained without considering short-circuit constraints, shown in the previous subsection for Case II, the maximum deviation of the short-circuit current value is 29.75%.

The average computational time to solve the problems in Case I is 46.16 s while for Case II, the average computational time is 1.23 h. The results were validated using a power flow algorithm and it was verified that the operation of all of them is feasible.

The obtained results indicate that the proposed formulation is capable of obtaining configurations that reduce the total annual cost of the energy losses while maintaining adequate levels of short-circuit currents in the system.

3.4 Performance Comparison

This subsection presents performance tests of the proposed model according to the number of stochastic and short-circuits scenarios considering a maximum short-circuit current deviation

of 7%. Table III presents the number of scenarios and the CPU time needed to find the optimal solution to the problem. As expected, the results show that the solution time increases considerably when the number of scenarios increases. Note that, each stochastic scenario increases the model size in $2|\Omega_N| + 5|\Omega_B| + 2|\Omega_{SS}| + 2|\Omega_{DG}|$ variables and in $3|\Omega_N| + 8|\Omega_B| + |\Omega_{SS}| + 4|\Omega_{DG}|$ constraints, of which $3|\Omega_N| + 7|\Omega_B| + 3|\Omega_{DG}|$ are linear constraints, $|\Omega_{SS}| + |\Omega_{DG}|$ are quadratic constraints, and $|\Omega_B|$ are second-order cone constraints, as can be verified in (2)–(16), while each short-circuit scenario only increases the model size in $4|\Omega_{\mathcal{N}}| + 4|\Omega_{\mathcal{B}}| + 2|\Omega_{SS}|$ variables and in $2|\Omega_{\mathcal{N}}| + 5|\Omega_{\mathcal{B}}|$ constraints, of which $2|\Omega_{\mathcal{N}}| + 4|\Omega_{\mathcal{B}}|$ are linear constraints and $|\Omega_{\mathcal{B}}|$ are quadratic constraints, as it can be verified in (21)–(27).

4. Conclusion

This work presented a novel mixed-integer second-order cone programming model for the distribution network reconfiguration problem considering short-circuit constraints. The scenario-based stochastic formulation accounted for the uncertainty of the demand, renewable generation, and energy prices.

Tests were carried out using an 84-node system, and the results indicated that the proposed formulation is capable of providing high-quality solutions for the problem while maintaining the short-circuit currents of the system within acceptable ranges, complying with the isolation levels of equipment, and trying to maintain the coordination of the system protection.

Future works will consider other objectives in the problem, such as increasing the hosting capacity of the network. Moreover, a three-phase unbalanced representation of the network operation can be used for both normal operation and the calculation of short-circuit currents. The proposed short-circuit constraints will also be included in the service restoration problem so that the protective devices can adequately actuate in the case of a fault in the network during the restorative state for the configurations provided by the restoration model.

5. Acknowledgment

This work was supported by the Coordination for the Improvement of Higher Education Personnel (CAPES) – Finance Code 001, the Brazilian National Council for Scientific and Technological Development (CNPq), grants 305852/2017-5, 304726/2020-6, and 408898/2021-6, and the São Paulo Research Foundation (FAPESP), under grants 2015/21972-6, 2018/20355-1, 2019/01841-5, 2019/23755-3, and 2021/08832-1.

J. P. S. Catalão acknowledges the support by FEDER funds through COMPETE 2020 and by Portuguese funds through FCT, under POCI-01-0145-FEDER-029803 (02/SAICT/2017).

References

[1] Gönen T. Electric power distribution system engineering. 2nd ed. Boca Raton, FL, USA: CRC Press; 2008.

[2] Lavorato M, Franco JF, Rider MJ, Romero R. Imposing radiality constraints in distribution system optimization problems. IEEE Transactions on Power Systems 2012;27:172–80. https://doi.org/10.1109/TPWRS.2011.2161349.

[3] Ritter D, Franco JF, Romero R. Analysis of the radial operation of distribution systems considering operation with minimal losses. International Journal of Electrical Power & Energy Systems 2015;67:453–61. https://doi.org/10.1016/j.ijepes.2014.12.018.

[4] Foltyn L, Vysocký J, Prettico G, Běloch M, Praks P, Fulli G. OPF solution for a real Czech urban meshed distribution network using a genetic algorithm. Sustainable Energy, Grids and Networks 2021;26. https://doi.org/10.1016/j.segan.2021.100437.

[5] Alvarez-Herault MC, Doye N, Gandioli C, Hadjsaid N, Tixador P. Meshed distribution network vs reinforcement to increase the distributed generation connection. Sustainable Energy, Grids and Networks 2015;1:20–7. https://doi.org/10.1016/j.segan.2014.11.001.

[6] Chen T-H, Huang W-T, Gu J-C, Pu G-C, Hsu Y-F, Guo T-Y. Feasibility study of upgrading primary feeders from radial and open-loop to normally closed-loop arrangement. IEEE Transactions on Power Systems 2004;19:1308–16. https://doi.org/10.1109/TPWRS.2004.831263.

[7] Jacob RA, Zhang J. Distribution network reconfiguration to increase photovoltaic hosting capacity. 2020 IEEE Power & Energy Society General Meeting (PESGM), Montreal, QC, Canada: IEEE; 2020, p. 1–5. https://doi.org/10.1109/PESGM41954.2020.9281922.

[8] Santos SF, Fitiwi DZ, Shafie-Khah M, Bizuayehu AW, Cabrita CMP, Catalão JPS. New multistage and stochastic mathematical model for maximizing RES hosting capacity—Part I: problem formulation. IEEE Transactions on Sustainable Energy 2017;8:304–19. https://doi.org/10.1109/TSTE.2016.2598400.

[9] Vargas R, Macedo LH, Home-Ortiz JM, Romero R. Optimal restoration of distribution systems considering temporary closed-loop operation. IEEE Systems Journal 2021:1–12. https://doi.org/10.1109/JSYST.2021.3073941.

[10] Mishra S, Das D, Paul S. A comprehensive review on power distribution network reconfiguration. Energy Systems 2017;8:227–84. https://doi.org/10.1007/s12667-016-0195-7.

[11] Zheng W, Huang W, Hill DJ, Hou Y. An adaptive distributionally robust model for three-phase distribution network reconfiguration. IEEE Transactions on Smart Grid 2021;12:1224–37. https://doi.org/10.1109/TSG.2020.3030299.

[12] Shukla J, Panigrahi BK, Ray PK. Stochastic reconfiguration of distribution system considering stability, correlated loads and renewable energy based DGs with varying penetration. Sustainable Energy, Grids and Networks 2020;23. https://doi.org/10.1016/j.segan.2020.100366.

[13] Chicco G, Mazza A. Assessment of optimal distribution network reconfiguration results using stochastic dominance concepts. Sustainable Energy, Grids and Networks 2017;9:75–9. https://doi.org/10.1016/j.segan.2016.12.005.

[14] Meskin M, Domijan A, Grinberg I. Impact of distributed generation on the protection systems of distribution networks: analysis and remedies – review paper. IET Generation, Transmission & Distribution 2020;14:5944–60. https://doi.org/10.1049/iet-gtd.2019.1652.

[15] Liu Y, Fan R, Terzija V. Power system restoration: a literature review from 2006 to 2016. Journal of Modern Power Systems and Clean Energy 2016;4:332–41. https://doi.org/10.1007/s40565-016-0219-2.

[16] Vargas R, Macedo LH, Home-Ortiz JM, Mantovani JRS, Romero R. Optimal restoration of active distribution systems with voltage control and closed-loop operation. IEEE Transactions on Smart Grid 2021;12:2295–306. https://doi.org/10.1109/TSG.2021.3050931.

[17] Rueda-Medina AC, Franco JF, Rider MJ, Padilha-Feltrin A, Romero R. A mixed-integer linear programming approach for optimal type, size and allocation of distributed generation in radial distribution systems. Electric Power Systems Research 2013;97:133–43. https://doi.org/10.1016/j.epsr.2012.12.009.

[18] Chiou J-P, Chang C-F, Su C-T. Variable scaling hybrid differential evolution for solving network reconfiguration of distribution systems. IEEE Transactions on Power Systems 2005;20:668–74. https://doi.org/10.1109/TPWRS.2005.846096.

[19] LaPSEE power system test cases repository 2022. https://www.feis.unesp.br/#!/departamentos/engenharia-eletrica/pesquisas-e-projetos/lapsee/downloads/materiais-de-cursos1193/ (accessed May 4, 2022).

[20] Wu J. Advances in k-means clustering: a data mining thinking. 1st ed. Berlin, Germany: Springer-Verlag; 2012. https://doi.org/10.1007/978-3-642-29807-3.

[21] Fourer R, Gay DM, Kernighan BW. AMPL: A modeling language for mathematical programming. 2nd ed. Duxbury, MA, USA: Thomson; 2003.

[22] IBM. IBM ILOG CPLEX Optimization Studio 20.1.0 documentation 2021. https://www.ibm.com/support/knowledgecenter/SSSA5P_20.1.0/COS_KC_home.html (accessed January 31, 2021).